A&A 383, 352–359 (2002)
DOI: 10.1051/0004-6361:20011700

Astronomy & Astrophysics

Diffractive-refractive optics for high energy astronomy

II. Variations on the theme

G. K. Skinner[1,2,⋆]

[1] CESR, 9 avenue du Colonel Roche, 31028 Toulouse, France
[2] School of Physics and Astronomy, University of Birmingham, Edgbaston, Birmingham B15 2TT, UK

Received 25 September 2001 / Accepted 15 November 2001

Abstract. In a companion paper diffractive-refractive optics components such as Fresnel Zone Plates and their derivatives have been proposed as a basis for telescope systems for X-ray and gamma-ray astronomy with high sensitivity and superb angular resolution. A wide family of configurations is possible and the first paper concentrated on simple systems for gamma-ray energies. The main problems arise from the very long focal lengths involved ($\sim 10^6$ km) and from chromatic aberration in the focussing system. Ideas are presented here that could in some circumstances allow the focal length to be reduced by many orders of magnitude. In addition it is shown how lenses which are to first order achromatic might be constructed. Finally, the possibility of using similar optical components for X-ray and gamma-ray interferometry is discussed.

Key words. telescopes – methods: observational – techniques: interferometric – gamma-rays: observations – X-rays: general

1. Introduction

In a companion paper (Skinner 2001, Paper I), the possibility was discussed of using diffractive-refractive optics to overcome the limitations encountered in hard X-ray and gamma-ray astronomy due to limited sensitivity and poor angular resolution. It was shown that devices based on Fresnel Zone Plates (FZPs), in particular the Phase Fresnel Lens (PFL), show great promise in this respect. An example device working at 500 keV would consist of a simple aluminium disk just over 1 mm thick and perhaps 5 m in diameter with concentric circular profiled grooves. It could provide a factor of 10^3–10^4 improvement in sensitivity over present generation gamma-ray instruments and at the same time have an angular resolution at the microarcsec level – a factor of $>10^8$ improvement. The main difficulties arise through the very long focal lengths involved ($\sim 10^6$ km for the examples in Paper I) and the narrow energy range with a given detector plane position which results from the chromatic nature of the images. In addition, because of the extremely high angular resolution, a detector with a reasonable area and number of pixels corresponds to a very small field of view.

Variations on the theme of diffractive-refractive lenses are discussed here, particularly with a view to alleviating these limitations.

Gamma-ray lenses with large apertures and long focal lengths were stressed in Paper I because obtaining extremely high angular resolution was one of the objectives of the studies which led to the ideas presented there. The reduction of the focal length by using the finest possible groove spacing, by working at lower energies and by using smaller apertures are first discussed (Sect. 2). Among other possibilities, a novel technique, the coded zone plate array, which could allow all of these developments to be combined is presented (2.3). Sections 3 and 4 discuss ways in which the bandwidth could be increased, including the use of the equivalent of an achromatic doublet. Finally, the prospects for X-ray and gamma-ray interferometry using diffractive-refractive optics are discussed (Sect. 5).

2. Design considerations and the implications of reducing the focal length

The effective angular resolution of a PFL telescope with a lens of diameter d and focal length f operating at photon energy E, or wavelength λ, results from the combination of three blurring contributions:
(i) the diffraction limited angular resolution

$$\theta_{\rm d} = 1.22\lambda/d, \tag{1}$$

(ii) the detector spatial resolution limit

$$\theta_{\rm s} = \Delta x/f, \tag{2}$$

⋆ e-mail: skinner@cesr.fr

(iii) the chromatic aberration limit (see Paper I)

$$\theta_{\Delta E} = 0.2\,(\Delta E/E)\,(d/f). \quad (3)$$

Here Δx is the detector spatial resolution and ΔE is the energy bandwidth over which observations are made. Notice in particular how $\theta_{\Delta E}$ is inversely proportional to f/d, the f-number of the lens.

When the very best angular resolution is sought, simple choices of parameters lead to focal lengths of the order of 10^6 km. Particularly where one can accept resolution which is lower (but which may nevertheless be orders of magnitude better than the current state of the art), there may be grounds for reducing the focal length as much as possible. Not only are spacecraft operations simplified but the linear size of an image element, and hence the detector background noise, can be reduced and the field of view for a given detector size can be increased. Table 1 addresses the considerations.

The equation for the focal length

$$\begin{aligned} f &= p_{\min} d/2\lambda \\ &= 0.40 \times 10^6 \left(\frac{p_{\min}}{1\ \mathrm{mm}}\right)\left(\frac{d}{1\ \mathrm{m}}\right)\left(\frac{E}{1\ \mathrm{MeV}}\right)\ \mathrm{km} \end{aligned}$$

shows that f may be reduced by decreasing the finest pitch $p_{\min}$ (that at the periphery of the lens), by decreasing the lens diameter d, or by working at a lower energy E. The implications of these three possibilities are considered in the following sections.

2.1. Fine pitch PFLs

The extent to which the focal length can be reduced by using a finer pitch is limited by the technologies available for making the lens. For a given energy, the required thickness, $t_{\max} = t_{2\pi}$, depends on the material (it is approximately inversely proportional to the density), but is otherwise fixed (Paper I, Fig. 2). Thus a finer pitch implies a higher aspect ratio $t_{\max}/p_{\min}$.

Consider, for example the 5 m diameter 500 keV lens considered in Paper I. With the finest pitch $p_{\min} = 1$ mm discussed there, the focal length is 10^6 km. If $p_{\min}$ can be reduced to 50 μm the focal length would be a "mere" 50 000 km. As can be seen from Table 2b, with a reasonable bandwidth of 2.5 keV, chromatic aberration would degrade the angular resolution to 27 μ'' corresponding to a focal spot size of about 6 mm. Although now far from the diffraction limit, the angular resolution would still be 10^4 times better than the current state of the art. Point source sensitivity would be only slightly degraded and sensitivity to a resolved extended source would be enhanced by a factor ∼400.

If the lens were made out of aluminium, as assumed in Paper I, the aspect ratio would be 20 – a figure difficult to achieve with conventional manufacturing techniques. This can be reduced somewhat if a denser material is used; for example with Molybdenum $t_{\max}$ would be reduced to 335 μm, giving an aspect ratio of less than 7. Despite the higher Z, at 500 keV the absorbtion losses would only be marginally increased and would remain below 2%.

The lens could also be constructed by stacking a number of well aligned components, each component having a lower aspect ratio but such that the total thickness of material encountered by the radiation varies with radius in just the way required. This is essentially the technique which has been successfully used for purely refractive lenses at synchrotron facilities (Lengeler et al. 1999; Piestrup et al. 2000).

Among the technologies which might be considered for constructing a lens with a fine pitch and high aspect ratio are (a) diamond turning, (b) stereolithography and (c) stacking of photochemically machined grids. All of these are possible approaches. In particular (c) has already been successfully employed in a very similar application. It was used to produce grids for HESSI with 34 μm pitch and 1 mm thickness by stacking 15 μm etched Molybdenum foils (Desai et al. 1999). By stacking grids with different open-fraction, a stepped approximation to the required PFL profile (cf. di Fabrizio & Gentili 1999) could be obtained.

2.2. Lower energies: X-ray PFLs

To obtain microarcsec resolution in the X-ray band requires large diameters (30 m aperture at 10 keV, for example, and correspondingly larger diameters at lower energies). Diffractive lenses are simple and do not require precision alignment, so by using deployment systems devices on this scale are not inconceivable. For the highest angular resolutions it is more likely that interferometric systems with unfilled apertures would be used in this regime and how that might be done will be discussed separately below. However, where ultimate angular resolution is not the goal, working at X-ray energies allows PFLs of shorter focal length to be used.

For the purposes of defining an example system, a detector resolution of $\Delta E/E = 2\%$ has been assumed, consistent with what is achievable with silicon pixel detectors. The size of the illuminated spot on the detector is dictated by chromatic aberration (Eq. (3)).

Absorbtion is more important in X-ray lenses than in those for gamma-rays and in contrast to the situation at higher energies, low Z materials are significantly better than high Z ones. However, as can be seen from Table 2c, at 10 keV materials such as a polycarbonate plastic[1] are still reasonably efficient and the difficulty and expense of using materials like Beryllium are probably not justified.

The example in Table 2c, shows how the focal length can be vastly reduced (to 400 km with the parameters

[1] An interesting aspect of the use at ∼keV energies of lenses made from materials which are transparent in the visible or infrared is the possibility of testing them with radiation of a wavelength chosen such that the ratio δ/λ is identical to that in the X-ray band. The same focal spot size should be obtained, but with a focal length reduced by a factor of the order of 10^3.

Table 1. Implications of reducing the focal length.

Advantages	Disadvantages
Reduced gravity gradient forces	Chromatic abberation worse (or d, or $\Delta E/E$, reduced)
Larger field of view	Pointing determination by spacecraft position measurement more difficult
Better sensitivity (particularly to low surface brightness objects)	Angular resolution may be detector limited
	Lens manufacture more critical

Table 2. Some possible lenses with reduced focal length compared with an example lens discussed in Paper I.

	(a) e.g. from Paper I	(b) Fine Pitch	(c) Low Energy	(d) Small Diameter
Energy, E (keV)	500	500	10	10
Diameter d (m)	5	5	5	0.025[1]
Finest Pitch, $p_{\rm min}$ (μm)	1000	50	20	10
Focal length, f (km)	10^6	50 000	400	1
Material	Aluminium	Molybdenum	Plastic	Silicon
Thickness, $t_{\rm max}$ (μm)	1150	335	50	25
Aspect ratio $t_{\rm max}/p$	1.2	7	2.5	2
Losses				
Absorbtion	1.3%	1.5%	8%	9.5%
Due to stepped approximation				18%
Detector plane				
Assumed ΔE (keV)	2.5	2.5	0.2	0.2
Assumed pixel size Δx (mm)	2	2	2	0.025
Angular resolution[2]				
Diffraction limit, $\theta_{\rm d}$	0.13 μ''	0.13 μ''	6 μ''	1.2 m$''$
Detector limit, $\theta_{\rm s}$	0.41 μ''	8 μ''	1 m$''$	5 m$''$
Chromatic aberration, $\theta_{\Delta E}$	1.28 μ''	26 μ''	13 m$''$	25 m$''$
Total, $\theta_{\rm tot}$	1.35 μ''	27 μ''	13 m$''$	26 m$''$
Field of view				
per m of detector	200 μ''	4 m$''$	0.5 $''$	200 $''$
Sensitivity[3]				
Continuum (Photons cm^{-2} s^{-1} keV^{-1})	3×10^{-10}	3×10^{-10}	4×10^{-9}	8×10^{-8}
Narrow line (Photons cm^{-2} s^{-1})	1.5×10^{-9}	1.5×10^{-9}	4×10^{-10}	1×10^{-8}
Diffuse narrow line (Photons cm^{-2} s^{-1} sr^{-1})	1.3×10^{13}	3.3×10^{10}	3×10^{5}	1×10^{6}

Notes:
1. Stepped; an array of 1024 such lenses in a CZP (Sect. 2.3) is assumed in the sensitivity calculations.
2. Microarcsec (μ'') or milliarcsec (m$''$).
3. Sensitivity calculations are for 5σ in one resolution element in 10^6 s and assume a background of 5×10^{-6} events cm^{-2} s^{-1} keV^{-1} at 500 keV and 2×10^{-4} events cm^{-2} s^{-1} keV^{-1} at 10 keV.

assumed), although with the smaller f-number chromatic aberration leads to angular resolution degraded to the milliarcsec level.

2.3. Small diameter PFLs: The coded zone plate array

Particularly at X-ray energies, relatively short focal lengths can be obtained if the lens diameter is modest. As an example we consider a lens with the parameters in Table 2d which correspond to focal length of 1 km, though the lens diameter would be only 25 mm. A 4-level stepped PFL with an aspect ratio (thickness/pitch) of ∼2 made from silicon has been assumed, although plastic or other materials could also be used.

Such a lens might have a high efficiency. For a 150 μm diameter stepped lens working at 7 keV, di Fabrizio & Gentili (1999) have measured 55% efficiency compared with a theoretical value of 72% showing that, even when

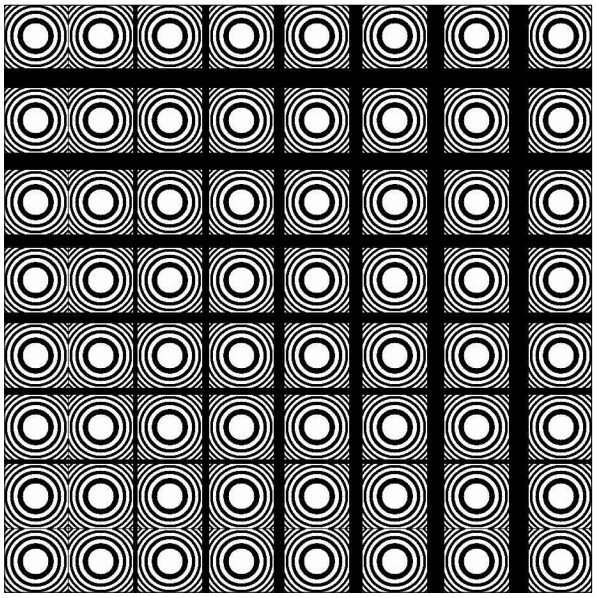

Fig. 1. A coded zone plate array constructed using the placing algorithm in Eq. (7). The zone plates could be increased in size to fill the gaps but this is not shown here to make the construction more apparent.

working on a small scale requiring sub-micron precision, performance not far from the theoretical limit can be achieved.

The effective area of a single lens with the parameters in Table 2d would be too small for most astronomical applications. However, without entering here into detailed consideration of fabrication techniques, mass production of such lenses and the assembly of a large array of lenses is certainly conceivable and we will consider here the use of such an array.

Consider an array of identical FZP (or PZP or PFL) lenses specified by $A(x, y)$ which contains a δ-function at each position where a lens is centred. The resulting image recorded in the focal plane will be

$$I = P \odot S = (A \odot P_0) \odot S \tag{4}$$

where P is the point source response function (PSF) of the compound lens, P_0 that of an individual lens and $\odot$ is the convolution operator. Addition of intensities rather than complex amplitudes is assumed here for simplicity and because, assuming that the typical separation between lenses is greater than the size of a single lens, interference effects will give rise to structure only on a scale finer than than the core of the PSF.

Equation (4) implies that there will be ambiguities in the image arising from the multi-peaked nature of $A \odot P_0$. If A represents a regular grid, there is little which can be done to resolve that ambiguity. The problem is similar to that of decoding the image recorded in the detector plane of a coded mask telescope where the images cast by different holes in the mask, each acting as the pinhole in a pinhole camera, overlap. Suppose now that A is not simply a regular rectangular grid but that each lens, i, is at a position $\boldsymbol{a_{ij}}$, which is allocated either randomly or according to some algorithm. As with a coded mask telescope, a good estimate of the object field can be obtained by performing a correlation between the observed flux distribution and A:

$$\begin{aligned} \hat{S} &= A \odot I = A \odot (A \odot P \odot S) \\ &= ACF(A) \odot (P \odot S). \end{aligned} \tag{5}$$

Thus the effective PSF of the system as a whole (hardware plus post-processing) is like that of a single lens, except that it is convolved with the autocorrelation function, $ACF(A) = A \odot A$.

The effective PSF will have sidelobes which reach to height n/N of the central peak, where a signal is detected from N individual lenses and where a particular vector separation $\boldsymbol{a_{ij}} - \boldsymbol{a_{kl}}$ between lens centres is repeated up to n times. Separations should be considered distinct if they differ by more than size of the focal spot, $s_\mathrm{d} = f\theta_\mathrm{d} = 0.61p$ (from Eqs. (1), (3))[2]. The problem of choosing the array A to minimise the number of repeated separations is related to those of designing coded mask patterns and of laying out radio interferometer arrays (Golay 1971; Kopilovich 1998). For the present purposes a possible algorithm is

$$\boldsymbol{a_{ij}} = (id + i^2 s_\mathrm{d})\, \boldsymbol{x_0} + (jd + j^2 s_\mathrm{d})\, \boldsymbol{y_0}, \tag{6}$$

where $\boldsymbol{x_0}, \boldsymbol{y_0}$ are unit vectors. In this case

$$\begin{aligned} \boldsymbol{a_{ij}} - \boldsymbol{a_{kl}} = \; & (i-k)\left(1 + (i+k)\tfrac{s_\mathrm{d}}{d}\right)\, d\, \boldsymbol{x_0} \\ + \; & (j-k)\left(1 + (j+l)\tfrac{s_\mathrm{d}}{d}\right)\, d\, \boldsymbol{y_0} \end{aligned} \tag{7}$$

and provided $(i + k)s_\mathrm{d}/d < 1$ each vector separation will only occur once and the highest sidelobe will have height $1/N$. For large N this means that the imaging performance is essentially that of a single lens, while the sensitivity will be $N^{1/2}$ times better.

Because of the small thickness needed to produce the required phase shifts, it should be possible to reduce the pitch to the point where the diffraction limited spatial resolution is well matched to the pixel size. In the example given in Table 2d the pixel size and energy resolution possible with large format CCDs are assumed. An array of such detectors would be needed. Although the angular resolution and sensitivity could never be as good as with a large single long focus lens they are nevertheless competitive with what is possible in other ways and the focal length can be reduced to ∼1 km.

3. Multi-energy lenses

PFLs can operate at any energy over a wide range by moving the detector to the appropriate focal plane, as was shown in Paper I. However because of chromatic aberration, for a given detector position the energy response is

[2] For simplicity it is assumed here that the system is diffraction limited.

quite restricted. We consider now ways in which the same lens can operate at more than one energy simultaneously.

A simple approach would be to divide the area of the lens into regions, for example into sectors, with a subset of the regions allocated to focussing each of a number of different energies onto the same focal plane. Multiple energies could be focussed, but at the expense of reduced effective area at each energy and of a slight degradation of the point source response function, due to the incompletely filled aperture.

Even a PFL with its whole surface area perfectly optimised for one energy naturally has some response at certain other energies. A PFL can be considered as a variable pitch grating which is blazed by arranging that each cycle is a prism directing the radiation towards the order $n = +1$. Consider a lens designed for energy E_1 (wavelength λ_1) at which the real part of the refractive index is $\mu_\mathrm{r} = 1 - \delta_1$. For radiation of energy $E_2 = n\,E_1$, where n is an integer greater than 1, at which $\mu_\mathrm{r} = 1 - \delta_2$, the the order n focus will be be at the same distance f. Ignoring absorption losses, the fraction of energy which goes into this focus is $I = AA^*$, where

$$A = \frac{1}{p}\int_{r_0}^{r_0+p} \exp\Big[\frac{2\pi i}{\lambda_2}\Big(t(r)\delta_2 - \frac{r(r-r_0)}{f}\Big)\Big]\mathrm{d}r. \qquad (8)$$

The integration may be over any complete cycle of the sawtooth profile and it has been assumed that r is large for simplicity. Putting in the thickness profile

$$t(r) = \frac{r(r-r_0)}{f\delta_1}, \qquad (9)$$

which is ideal at energy E_1, and using the fact that at high energy $\delta_{nE} = \delta_E/n^2$ and the value $f\lambda_1/r_0$ for p (Eq. (4)), one finds

$$\begin{aligned} A &= \frac{1}{p}\int_{r_0}^{r_0+p} \exp\Big[\frac{2\pi i}{\lambda_1}\frac{r(r-r_0)}{f}\big(\frac{1}{n} - n\big)\Big]\mathrm{d}r \\ &= \frac{\exp(-2\pi i\big(n - \frac{1}{n}\big)) - 1}{2\pi(n - \frac{1}{n})}\, i. \end{aligned}$$

This is non-zero for all n, showing that even an ideal lens which puts all the flux at the nominal energy E_1 into the first order focus at distance f will put some of the flux at energy $E_2 = 2E_1$ and at $E_3 = 3E_1$, etc. into the $n = +2, +3, \ldots$ focii for these energies. So a detector at the nominal focal plane will be able to receive weak images at integer multiples of the nominal energy. The efficiency will, however, be low (Table 3, Col. c).

One can, however, do better. Adding over part of the surface of a PFL a layer of thickness $k\lambda_1/\delta_1 = kt_{2\pi}$, for any integer k, will not affect the performance at energy E_1 except for some increased absorption losses which may not be too serious if $kt_{2\pi}$ is not too large. Thus a Phase Zone Plate (PZP) for another wavelength can be added in front of the PFL while scarcely affecting the performance at the nominal energy. This leads to the structure illustrated in Fig. 2. The focal plane of the PZP at its design energy E_2 can be the same as that of the PFL at E_1. The concept

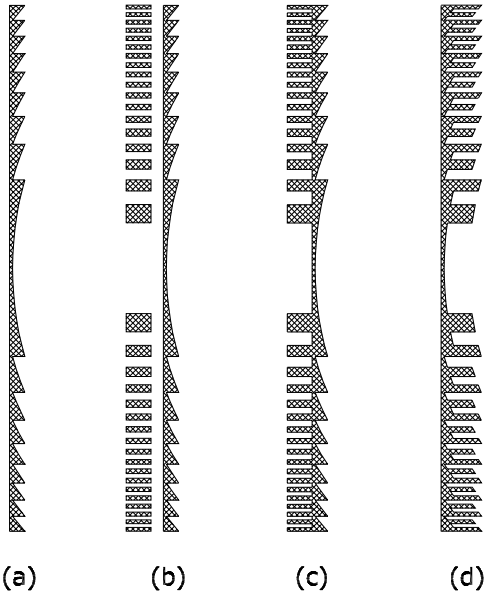

Fig. 2. The development of a lens for two energies by adding to the basic PFL in **a)** material as shown in **b)** which produces a integral number of wavelengths shift at the nominal energy. The additional material which forms a PZP at a different energy can be part of the PFL as in **c)** and if desired a single combined pattern could be used as in **d)**. The case illustrated is $k = 2$, $m = 2$, corresponding to $E_2 = 2E_1$.

Table 3. The efficiency at different energies of lenses using the principle in Fig. 2 compared with that of a simple PFL. The 500 keV example from Paper I is used used as a basis. The PZP pitch is m times smaller that that of the PFL.

(a)	(b)	(c)	(d)	(e)	(f)
Energy	keV	PFL	PFL plus PZP		
			$k=1$	$k=2$	$k=2$
			$m=2$	$m=3$	$m=4$
E_nom	500	98.7%	98.7%	98.6%	98.6%
$2E_\mathrm{nom}$	1000	4.4%	24.5%		
$3E_\mathrm{nom}$	1500	1.0%		29.6%	
$4E_\mathrm{nom}$	4000	0.3%			35.3%

naturally leads to combinations of E_1 and E_2 which are in simple ratios (e.g. Table 3), but other ratios can be accommodated with minimal reduction in efficiency.

The efficiency of a PZP is not as good as that of a PFL, being limited to 40.4%, and the presence of the PFL leads to further phase shifts which reduce the efficiency compared to an ideal PZP. But useful additional performance can be obtained with virtually no impact on the performance of the basic PFL (see Table 3).

4. Correcting chromatic aberration

The PFL depends heavily on refraction as well as on diffraction. It can be considered either as a refractively

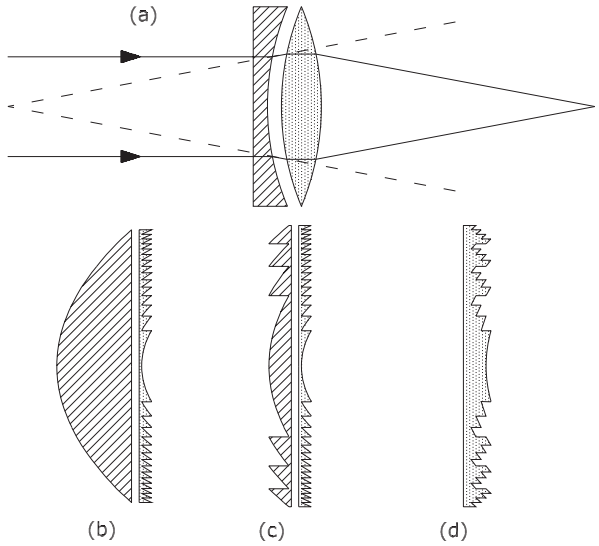

Fig. 3. a) The visible-light analogue of the proposed achromatic system – a diverging, high dispersion lens compensates the dispersion in a stronger converging lens. **b)** An X-ray or gamma-ray equivalent, which would, however, suffer from strong absorption. **c)** Reducing the absorption by removing layers of material. **d)** Combining the two components.

blazed variable pitch grating as above, or as a refractive lens in which the thickness is reduced by removing layers of material whose thickness is such that they correspond to a phase shift which is a multiple of 2π.

As was noted in Paper I, in some circumstances long focal length refractive lenses could be made and used instead of diffractive ones. But, as well as having high absorbtion losses, such lenses would suffer even more from chromatic aberration than their diffractive-refractive equivalent, the focal length being proportional to E^2 instead of to E. This different energy dependence suggests the possibility of making an achromatic pair as illustrated in Fig. 3.

If the focal lengths of the two lens components in Fig. 3 are in the ratio -2:1, then to first order dispersion effects cancel and the focal length of the combination at energy $E + \Delta E$ is

$$f = 2f_{\rm d}\left[1 + \left(\frac{\Delta E}{E}\right)^2 - 2\left(\frac{\Delta E}{E}\right)^3 + \ldots\right], \qquad (10)$$

where $f_{\rm d}$ is the focal length of the PFL component.

In practical cases the absorption losses in the refractive component in Fig. 3b would usually be prohibitive. The possibility exists, however, of reducing the thickness modulo some thickness $t_{\rm r}$ as illustrated in Figs. 3c,d. Suppose $t_{\rm r} = mt_{2\pi}(E_{\rm nom})$ for some moderately large integer m, where $t_{2\pi}(E_{\rm nom}) = \delta(E_{\rm nom})/\lambda(E_{\rm nom})$ is the thickness required to give a phase shift of 2π at the nominal design energy E_1. The focussing properties at the nominal energy $E_{\rm nom}$ will be unchanged, but so will those for any other energy E at which $t_{\rm r} = m't_{2\pi}(E)$. Taking $\delta \propto E^2$ implies $t_{2\pi} \propto E$ and one finds that correct focussing in the nominal focal plane will occur for a comb of energies within the band for which the 2nd order and higher terms in Eq. (10) are negligible and with an energy spacing $\sim E_{\rm nom}/m$.

The performance predicted for an example system based on these ideas and with the parameters given in Table 4 is shown in Fig. 4. The scheme is of greatest interest when the absorbtion is low such that high values of m can be used without the absorbtion losses becoming too serious. This is the case for low Z materials and at hard X-ray energies, the lowest absorbtion in thickness $mt_{2\pi}(E)$ for a given m occurring at E from $\sim$15 keV for beryllium up to $\sim$80 keV for materials such as aluminium. For the example, a Polycarbonate lens working at 20 keV with $m = 200$ has been assumed. This has a maximum thickness of 19 mm.

Between the energies at which the correction works best, the focal spot is spread into a disk, over which a complex annular fringe structure extends. Thus a detector which is considerably larger than the diffraction limited focal spot size, but which nevertheless may be physically quite small, can collect most of the flux incident on the lens within the band pass of the achromat[3]. Where the absorbtion losses allow, high values of m are to be preferred – if the peaks are closely spaced a small detector can collect most of the flux at the "worst case" energies midway between them. In the example in considered here, a 30 mm diameter detector can receive an average of 55% of the flux falling on a 5 m diameter lens over a bandwidth of 3.7 keV centred on 20 keV.

The net response to a continuum source is increased by a factor 6–9, depending on the detector size assumed. Even after allowing for the fact that the detector background will be larger in the $\sim$10 times greater bandwidth, the sensitivity to a continuum source can be expected to be improved by a factor 2 (more for photon limited operation).

5. Interferometry using diffractive-refractive optics

In circumstances where angular resolution is of more importance than collecting area, interferometry is likely to be preferable to the use of a filled aperture direct imaging system. Such circumstances are more likely to arise in the X-ray band than with gamma-rays because at the lower energies photons are more abundant while the aperture size necessary for a given angular resolution is larger. Furthermore, at lower energies it may be simply impracticable to construct a filled aperture system of a size large enough to achieve microarcsec resolution or better.

The studies for MAXIM have identified a way in which an X-ray interferometer system might be assembled in space (Cash 2000). The MAXIM concept uses grazing incidence mirrors to combine the beams but it is worth considering whether diffractive-refractive optics might

[3] A detector with sufficiently good spectral and energy resolution to record the fringes would move such an instrument into the domain of interferometry, discussed in Sect. 5 below.

Table 4. Parameters for an example refractive/diffractive achromatic doublet.

Nominal energy, $E_{\rm nom}$	20	keV
Material	Polycarbonate	
Diameter, d	5	m
Diffractive (PFL) component		
Finest pitch p	0.5	mm
Maximum thickness $t_{2\pi}$	95	μm
Focal length	$+2 \times 10^7$	m
Mean absorbtion[1]	0.3	%
Refactive component		
Step factor m	200	
Thickness reduced modulo	18.9	mm
Focal length (m)	-4×10^7	m
Mean absorbtion	41.2	%
Combination		
Focal length (m)	$+4 \times 10^7$	m
Mean absorbtion	41.4	%

Note: 1. Absorbtion losses are given at $E_{\rm nom}$.

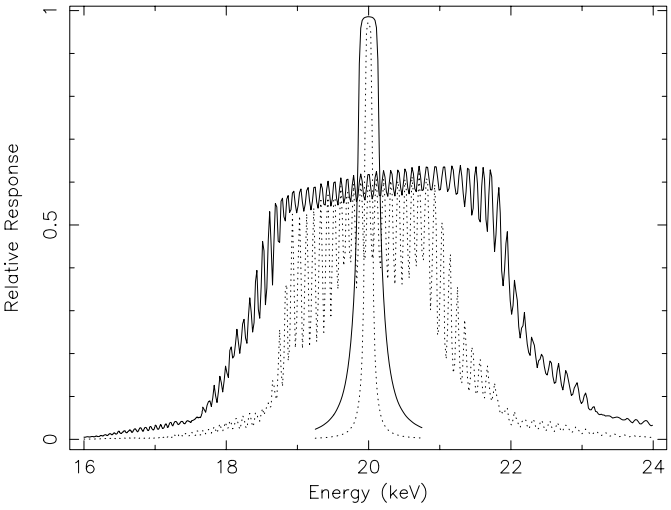

Fig. 4. Efficiency as a function of energy for the achromatic lens described in Table 4. The full line show the response for a 30 mm diameter detector and the dotted line that for a 10 mm diameter one. The narrow peaks are for a simple PFL with the same focal length. The effect of decreasing absorbtion as the energy increases can be seen as a slope to the "flat" top.

provide an alternative way of doing this. Chromatic effects preclude the use of pure refractive or pure diffractive devices – for different energies the beams would cross at very different positions (Fig. 5), but the achromatic scheme proposed in Sect. 4 provides a possible solution to this problem too, as shown in Figs. 6, 7.

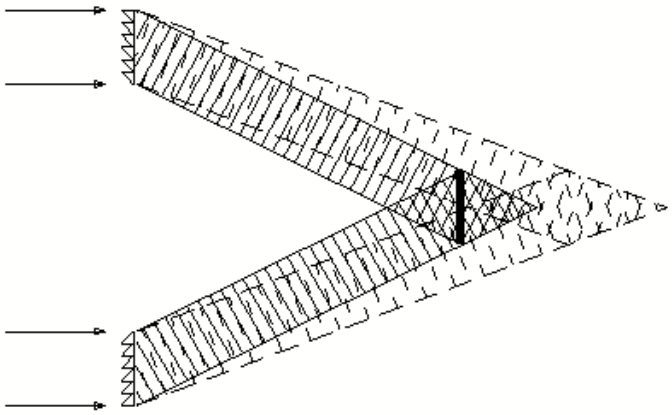

Fig. 5. An interferometer using a diffractive-refractive beam combiner.

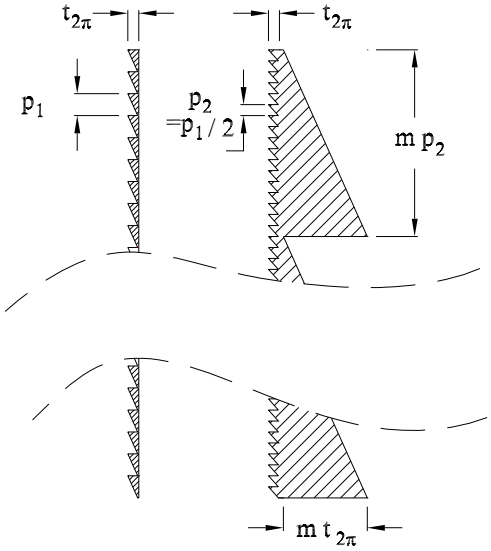

Fig. 6. a) The simple grating beam combining element illustrated in Fig. 5. **b)** A diffractive + refractive variation which would have much reduced chromatic effects. A component profiled on one side only with the same dependence of thickness with distance, analogous to Fig. 3d, might equally be used.

Although an interferometer based on these principles could be built for photon energies anywhere from a few keV to ∼a few MeV, the most favourable part of the spectrum for such an instrument is probably at energies of a few tens of keV. Table 5 shows what might be involved in obtaining 1 microarcsec resolution at 20 keV.

Simulations show that, apart from the additional absorbtion due to the increased thickness, the only adverse effect of adding the refractive component is a periodic modulation of the amplitude of the fringe pattern which occurs at certain specific energies due to beating between the two periods in the structure.

The principle advantage of this approach is that the beam deviations are relatively insensitive to the orientation of the deviating device. A small misalignment, α, of a

Table 5. Example Interferometer parameters. Each grating is assumed to be 500×500 mm. Figures marked by an asterisk apply at 20 keV.

Band (50% response)	18–22.5	(keV)
Length	10^5	(km)
Baseline	20 3.3×10^{12}	(m) (λ)
Material	Polycarbonate	
Fine pitch p_2	0.31	(mm)
Coarse pitch, mp_2	31	(mm)
Diffractive component steps $t_{2\pi}$	94	(μm)
Maximum Thickness	0.95	(mm)
Absorbtion losses*	22	(%)
Fringe spacing	0.31 0.64	(mm) (μ'')
Effective area* (per pair of gratings)	2400	(cm^2)

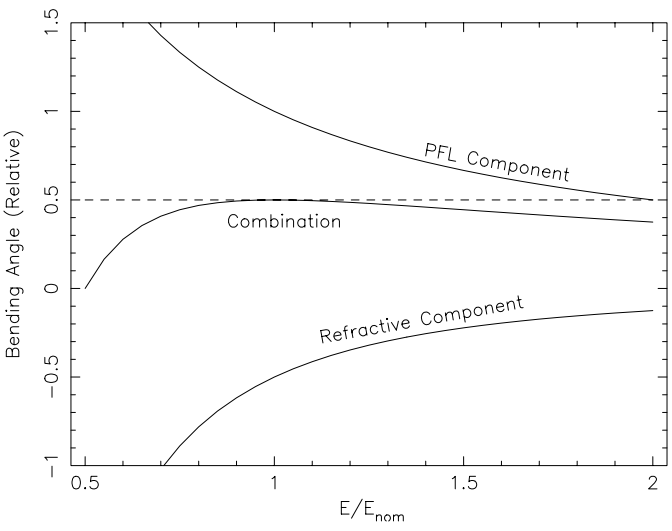

Fig. 7. The deflection angle as a function of energy, E, for a simple grating as used in a PFL, for a refractive prism, and for the combination shown in Fig. 6. The angle is relative to that of a simple grating at the nominal energy $E_{\rm nom}$.

mirror changes the alignment of the deviated beam by 2α, necessitating precision alignment. In contrast, errors in the alignment of the diffractive-refractive beam combiner have, to first order, no effect on the diffraction pattern.

Clearly longer combining elements could be used to enable a wider band of energies to be concentrated on the detector or other pairs of elements could be added. Additional pairs could work at the same energy but provide baselines with different orientations, adding their fringe patterns coherently. Alternatively they might be designed for different energies and have either the same or differently oriented baselines.

6. Conclusions

The concepts presented show how problems associated with long focal lengths and limited bandwidth can be considerably reduced by considering variations on the basic PFL design.

Some additional complexity is introduced compared with the very simple profiled plate PFLs presented in Paper I, but the components required are still comparatively simple and share with simple PFLs the same tolerance to misalignments. Some compromises are involved – in angular resolution if X-rays are used, in bandwidth if fine pitches lead to a smaller f-number, in background noise in the case of CZPs, and in additional absorbtion losses at the nominal energy in the case of achromatic lenses. However in the appropriate circumstances, the advantages offered could certainly outweigh all such limitations.

The wide variety of systems which may be considered starting from simple PFLs have been illustrated by the example concepts presented here. Instrument parameters which might be of interest have been chosen to illustrate the concepts. Certainly many more variations and combinations of the techniques need to be considered and other regions of parameter space should be explored. Particularly in the case of interferometry, only a general concept has been introduced and more work is needed in order to establish the optimum configuration and parameters. It is hoped that the ideas presented here will inspire such studies.

Acknowledgements. The author is again grateful for helpful comments and suggestions from many colleagues.

References

Cash, W. 2000, IAU Symp., 205, 38
Desai, U. D., Orwig, L. E., Clark, D., & Appleby, M. 1999, in Proc. SPIE, Micromachining and Microfabrication Process Technology V, ed. H. J. Smith, & J. M. Karam, 3874, 321
di Fabrizio, E., & Gentili, M. 1999, J. Vac. Sci. Tech. B, 17, 3439
Golay, M. J. E. 1971, J. Opt. Soc. Am., 61, 272
Kopilovich, L. E. 1998, J. Mod. Opt., 45, 2417
Lengeler, B., Schroer, C., Tümmler, J., et al. 1999, J. Synchroton Rad., 6, 1153
Piestrup, M. A., Cremer, J. T., Beguiristain, H. R., Gary, C. K., & Pantell, R. H. 2000, Rev. Sci. Instrum., 71, 4375
Skinner, G. K. 2001, A&A, 375, 691